International Journal of Applied Earth Observation and Geoinformation 132 (2024) 103962

Contents lists available at ScienceDirect

International Journal of Applied Earth Observation and Geoinformation

journal homepage: www.elsevier.com/locate/jag

Precipitation nowcasting using transformer-based generative models and transfer learning for improved disaster preparedness

Md. Jalil Piran [a], Xiaoding Wang [b], Ho Jun Kim [c], Hyun Han Kwon [c,*]

[a] Department of Computer Science, Sejong University, Seoul, 05006, Seoul, South Korea
[b] College of Computer and Cyber Security, Fujian Normal University, Fujian, 350117, China
[c] Department of Civil and Environmental Engineering, Sejong University, Seoul, 05006, South Korea

ARTICLE INFO

Keywords:
Precipitation nowcasting
Transformer-based generative model
Radar reflective data
ConvLSTM
cGAN
U-net

ABSTRACT

Due to the rapidly changing climate conditions, precipitation nowcasting poses a daunting challenge because it is impossible to make accurate short-term forecasts due to the rapid fluctuations in weather conditions. There are limitations to traditional methods of forecasting precipitation, such as the use of numerical models and radar extrapolation, when it comes to providing highly detailed and timely forecasts. With the help of contemporary machine learning (ML) models, including deep neural networks, transformers and generative models, complex precipitation nowcasting tasks can be performed in an efficient way. To address this critical task and enhance proactive emergency disaster management, we propose an innovative method based on transformer-based generative models for precipitation nowcasting. Our study area is the Soyang Dam basin in South Korea, located upstream of the Han River, characterized by a monsoon climate with approximately 1200 mm of annual precipitation. To develop a precipitation nowcasting model, radar composite data from 10 weather radars across South Korea is used. By utilizing radar reflective data in order to train our model, we are able to effectively predict future precipitation patterns, thus mitigating the risk of catastrophic weather conditions caused by heavy rainfalls. This dataset covers reflectivity data from 2018 to 2022, with a spatial resolution of 1km over a 960 × 1200 grid. Normalization using the min–max scaler method is applied to this reflectivity data, which is then transformed into grayscale images for uniform comparison. We enhance performance effectively by employing transfer learning with pre-trained Transformer models. Initially, we train the model using a comprehensive dataset. Subsequently, we fine-tune it for precipitation nowcasting using radar reflective data. This adaptation improves the accuracy of rainfall forecasting by capturing crucial features. Leveraging prior task knowledge through transfer learning not only enhances prediction accuracy but also increases overall efficiency. In terms of predictive accuracy, extensive experimental results demonstrate that our transformer-based nowcasting model outperforms related approaches, including conditional generative adversarial networks (cGANs), U-Net, convolutional long short-term memory (ConvLSTM), pySTEP. As a result of this research, disaster preparedness and response will be greatly improved through improved weather prediction.

1. Introduction

There has never been a more critical time to implement effective risk management strategies than now, as we face an increasing number of small-scale disasters (Fraser et al., 2020). It is becoming increasingly difficult to predict the weather patterns and to respond to imminent weather-related threats due to climate change and unpredictable weather patterns. Accurate predictions is especially helpful when dealing with immediate weather-related issues and activities (Ahamed and Bolten, 2017; Butsch et al., 2023).

Nowcasting is a technique that is used in the meteorological field to predict the weather conditions in the near future (Zhao et al., 2024). It is especially valuable in the case of short-term weather events like thunderstorms, torrential rains, snowfalls, and other types of precipitation that can last for a short period of time. As a useful tool in the realm of meteorology as well as in emergency preparedness, nowcasting has emerged as an essential component to the successful management of associated risks. Due to its unique capability to provide short-term weather forecasts, often at a mesoscale or local level, the Meteorological Service has proven invaluable in a variety of applications (Schmid et al., 2019). In order to track rapidly changing weather

* Corresponding author.
E-mail address: hkwon@sejong.ac.kr (H.H. Kwon).

https://doi.org/10.1016/j.jag.2024.103962
Received 18 April 2024; Received in revised form 29 May 2024; Accepted 6 June 2024
Available online 1 July 2024
1569-8432/© 2024 The Authors. Published by Elsevier B.V. This is an open access article under the CC BY-NC-ND license (http://creativecommons.org/licenses/by-nc-nd/4.0/).

patterns at a fine scale, nowcasting makes use of high-resolution data from sources such as radar data, satellite imagery, weather station observations, and other sources of high-resolution data in order to track fast-changing weather patterns at a fine scale (Cao et al., 2023). This technique involves combining real-time weather measurements, such as radar data, in order to track the movement and intensity of precipitation, storm cells, and other short-term weather phenomena by combining actual weather data with real-time weather measurements. Every few minutes, as new data becomes available, nowcasting models are routinely updated to reflect the latest information. As a result, it is possible to continuously observe how the weather pattern changes over time. In order to provide a nowcast, a variety of methodologies are used, including numerical weather models, machine learning (ML), and classic observational techniques.

As a crucial component of early warning systems designed to mitigate the impact of severe weather events, precipitation nowcasting, in particular, stands out as a crucial component of rainfall prediction systems (Zhang et al., 2023). Precipitation nowcasting is essentially a subset of weather forecasting in which we are focusing on predicting rainfall for a short period of time. In order to prevent the devastation caused by heavy rainfall, landslides, and flash floods, it is essential that precipitation patterns are predicted in a timely and accurate manner. There is no doubt that in an era when extreme weather events are becoming more frequent and severe, integrating nowcasting into our risk management strategies has the potential to not only avert potential disasters, but is also a proactive way for our communities to be protected. Weather forecasting has become more precise and accessible as a result of technological advancements and the availability of real-time data. The National Weather Services plays a critical role in taking essential measures to reduce the impact of rapidly changing weather conditions (Ahmed et al., 2023).

As a crucial component of early warning systems designed to mitigate the impact of severe weather events, precipitation nowcasting, in particular, stands out as a crucial component of rainfall prediction systems (Zhang et al., 2023). Precipitation nowcasting is essentially a subset of weather forecasting in which we are focusing on predicting rainfall for a short period of time. In order to prevent the devastation caused by heavy rainfall, landslides, and flash floods, it is essential that precipitation patterns are predicted in a timely and accurate manner. There is no doubt that in an era when extreme weather events are becoming more frequent and severe, integrating nowcasting into our risk management strategies has the potential to not only avert potential disasters, but is also a proactive way for our communities to be protected (Zhu et al., 2020; Li et al., 2022). Weather forecasting has become more precise and accessible as a result of technological advancements and the availability of real-time data. I believe that the National Weather Service plays a critical role in taking essential measures to reduce the impact of rapidly changing weather conditions (Ahmed et al., 2023).

As a result of radar signals bouncing off precipitation, a ground-based radar can be used to determine the intensity of precipitation. The efficiency of the weather radar system can be viewed in terms of how well objects in the atmosphere are able to reflect the radar's radiation back towards the radar. As a consequence, this efficiency is quantified in terms of radar reflectivity as a measure of efficiency. This is a measure of what is referred to as radar reflectivity, which is the amount of transmitted power that is returned to the radar receiver after impacting precipitation, as compared to a reference power density at a unit distance from the radar antenna (Dinh et al., 2023). Precipitation targets are detected based on a variety of factors that influence the detection process. Particularly, the weather conditions between the radar and the target, the distance between the radar and the target, the features of the target, as well as the radar characteristics can all play an important role in influencing the accuracy of the prediction. Atmospheric conditions as well as the actual nature of a given target are generally unknown quantities in general. As a result, it is of utmost importance to develop a model that is capable of predicting precipitation accurately in the near future.

ML-based approaches have revolutionized weather forecasting by providing intelligent, accurate, and timely predictions using a data-driven approach (Guo et al., 2023). As a subset of ML, deep learning (DL) models have shown great promise for improving nowcasting accuracy by capturing complex patterns and correlations in weather data (Isola et al., 2017). Recently, a number of DL-based models have been proposed to predict weather such as conditional generative adversarial networks (cGANs), U-Net (Zannah et al., 2024), convolutional long short-term memory networks (convLSTMs), and pySTEP (Isola et al., 2017; Rüttgers et al., 2019; Khankeshizadeh et al., 2024).

In spite of the promising results of these proposed methods, we believe that the transformers can significantly enhance the efficiency of weather forecasting (Akwensi et al., 2024). In transformers, input data is processed using self-attention mechanisms rather than convolutional layers, which allows them to learn more expressive feature spaces. CNNs rely on fixed-size convolutional kernels, which may not effectively capture complex spatio-temporal patterns. Due to their inherent ability to attend to all input positions, transformers automatically handle long-range dependencies. In order to capture the temporal context of precipitation data, this is crucial. ConvLST and CNNs have local receptive fields, limiting their ability to model long-term dependencies. Input sequences can be processed parallel by transformers, making them more scalable for large datasets. For long sequences, CNNs and ConvLSTMs operate sequentially, which can be computationally expensive. A transformer weights input features according to their relevance to each other by using self-attention. The context of the situation can be captured in this way. In contrast, CNNs and ConvLSTMs do not have this intrinsic mechanism for maintaining attention. In the case of transformers, it is possible to fine-tune them with limited data in order to perform specific tasks. The advantage of transformers is that they are robust in different domains and are capable of generalizing well across different scenarios, which is advantageous in weather prediction as they are able to generalize well across different types of scenarios.

Since transformers provide important and helpful features that are essential for precipitation nowcasting, this paper proposes a transformer-based approach for constructing a precipitation nowcasting model based on radar reflective data in order to construct a precipitation nowcasting model for dam basins. It is very important to have a precise rainfall forecasting model in order to estimate urban water supplies and prevent floods when dealing with urban areas.

Furthermore, we apply Cost-Effective Computational Methods to the pre-trained Transformer model in order to optimize performance. The model is initially trained on extensive datasets, and then we adapt it for precipitation nowcasting using radar reflective data. In order to enhance the accuracy of rainfall forecasting by capturing the important features of pre-trained models, transfer learning can be utilized with pre-trained models. The prediction of precipitation can be made more accurate and efficient by utilizing the knowledge gained from previous tasks through transfer learning.

The main contributions of this paper can be summarized as follows. We investigate the Soyang Dam basin in South Korea, located upstream of the Han River, characterized by a monsoon climate with approximately 1200 mm of annual precipitation. To develop a precipitation nowcasting model, radar composite data from 10 weather radars across South Korea is used. This dataset covers reflectivity data from 2018 to 2022, with a spatial resolution of 1 km over a 960×1200 grid. Normalization using the min–max scaler method is applied to this reflectivity data, which is then transformed into grayscale images for uniform comparison.

We propose a novel method for predicting precipitation using Transformer-based generative model. This innovative approach leverages the capabilities of transformer-based models to enhance the accuracy and efficiency of precipitation nowcasting. By harnessing the power of transformers, our proposed method offers a novel solution for real-time precipitation forecasting, addressing the challenges posed by extreme weather events such as floods and landslides.

In addition, to increase the efficiency of our proposed model, mini-batch stochastic gradient descent (SGD) training is introduced. The technique has proven invaluable in optimizing neural networks and accelerating convergence. By dividing the training data into smaller batches, gradients can be computed more frequently, resulting in faster weight updates. Noise introduced by Minibatch SGD helps the model escape local minima and explore the loss landscape more effectively.

We utilize transfer learning with pre-trained Transformer models to boost performance effectively. Starting with comprehensive dataset training, we adapt the model for precipitation nowcasting with radar reflective data, improving rainfall forecasting accuracy by capturing essential features. Leveraging prior task knowledge through transfer learning not only enhances prediction accuracy but also increases efficiency.

According to extensive experiments, the accuracy of prediction, as measured by prediction accuracy, is significantly higher than any of the existing methods, including cGANs, U-Net, convLSTMs, pySTEP.

We validate that our model is capable of predicting future precipitation patterns with a high degree of accuracy, which can assist in reducing the risk of catastrophic floods caused by heavy rainfall in the future. Through the use of the proposed model, disaster preparedness and response can be significantly improved by improving weather forecasts.

The rest of the paper is organized as follows. Section 2 presents related work, followed by Section 3, which explains the proposed methodology in details. Section 4 describes the experimental results obtained from the proposed approach and compares it with the state-of-the-art existing methods. In Section 5 we explain about our achievements and research funding. Finally, Section 6 draws the conclusions.

2. Related work

As a result of precipitation nowcasting, it is possible to make high-resolution forecasts of precipitation up to several hours in advance. In the real world, precipitation nowcasting serves the practical needs of a variety of sectors that make decisions based on weather conditions. The traditional methods of operational nowcasting often rely on radar-based data to advect precipitation fields, but these methods struggle when it comes to capturing non-linear events like convective initiations, which are harder to estimate. Recently, DL methods have been used directly to predict future rain rates based on radar data. However, their lack of constraints leads to blurry nowcasts at longer lead times, owing to their lack of constraints.

There have been a number of models that have been proposed regarding the accuracy of weather nowcasts. Table 1 summarizes the related research work on precipitation nowcasting. In this section, we discuss them one by one as follows.

The authors in Berenguer et al. (2012) developed a rainfall prediction model based on numerical weather prediction (NWP). This approach relies on physically-based equations from atmospheric physics, resulting in high-resolution rainfall forecasts with extended lead times. Furthermore, in Poletti et al. (2019), Hwang et al. (2020), the authors introduced several techniques that combine NWP and radar-based models. This blending approach enhanced short-term flood forecasting, improving the accuracy of short-term rainfall predictions. Most importantly, the radar-based models (extrapolation) approach, employed by Berenguer et al. (2012), Bech and Chau (2012), Renzullo et al. (2017), focused on extrapolating radar data for short-term rainfall prediction (0–6 h). Such models outperform NWP models when forecasting rainfall in the short term.

The application of ML to precipitation nowcasting plays an important role, particularly in the case of extreme weather events. There are limitations to the use of traditional numerical methods, such as the numerical one-hour high-resolution rapid refresh (HRRR) prediction of National Oceanic and Atmospheric Administration (NOAA). However, there are DL models that have shown promise in this regard, such as U-Net, convolutional neural networks (CNNs), long short-term memory (LSTM), and Transformers. For instance, using U-Net, a type of CNN commonly used in image translation problems, researchers have achieved better predictions than traditional methods (Trebing et al., 2021). These models process high-resolution radar images to generate accurate and timely forecasts, aiding in effective adaptation to climate change and enhancing our ability to respond to extreme weather conditions.

Various research works have been carried out recently to showcase the capability of ML in providing reliable and accurate nowcasting models. In this regard, the authors in Shi et al. (2015) used a ConvLSTM model for predicting future rainfall intensity by modeling the weather forecasting as a spatio-temporal sequence forecasting problem. Isola et al. (2017), and Rüttgers et al. (2019) utilized generative adversarial networks (GANs) and cGAN architectures for image-to-image tasks in rainfall prediction. Such mentioned models enhanced image quality extracted from the satellite images and the overall quality of rainfall predictions.

Similarly, Choi et al. in Choi and Kim (2022), proposed a precipitation nowcasting model Rad-cGAN using cGAN based on radar reflective data. In another work in Ayzel et al. (2019), Ayzel et al. introduced a rainfall prediction model based on optical flow techniques. This model leveraged advanced observation data and is available as an open-source Python library, making it accessible for research and application. Similar to the aforementioned work, the authors in Pulkkinen et al. (2019), developed a probabilistic nowcasting, pySTEPS, a deterministic and probabilistic nowcasting application. pySTEPS stands out as an open-source Python library and could be applied effectively in various countries.

Some of the research works in the literature have focused their studies on developing radar-based weather nowcasting models. In this regard, Shi et al. (2015) implemented a radar-based model using ConvLSTM architecture to capture spatiotemporal correlations in rainfall data. It excelled at capturing correlations, outperforming optical flow-based models. Again, the authors in Agrawal et al. (2019) introduced the U-Net model, a fully connected CNN model designed for superior rainfall predictions. It demonstrated its effectiveness by surpassing traditional NWP models. Likewise, in Ravuri et al. (2021), the authors developed a deep generative model inspired by video GANs for convective cell prediction, significantly enhancing the quality of precipitation forecasts.

The authors in Tuyen et al. (2022) proposed RainPredRNN, a novel approach for precipitation nowcasting with weather radar echo pictures that combines the U-Net segmentation model and the PredRNN-v2 DL model. The work in Ayzel et al. (2020) introduced RainNet, a CNN-based model for precipitation nowcasting using radar images. RainNet was trained using high-quality weather radar data to predict continuous precipitation intensities with a 5-minute lead time. Mean absolute error (MAE) and critical success index (CSI), two standard verification criteria, have shown that RainNet performs much better than the benchmark models for all lead times up to 60 min.

Transformers, originally intended for the processing of natural language processing (NLP), excel in capturing long-range dependencies between nodes in the network (Rothman, 2021). The Transformer-based generative models have revolutionized precipitation nowcasting by effectively capturing temporal dependencies and handling spatial information, thus revolutionizing precipitation nowcasting. In line with the principles of natural language processing, these models rely on attention mechanisms to focus on critical features in the radar echo sequences. Using their autoregressive prediction capabilities, they are able to ensure consistency and coherence in their predictions. In recent years, researchers have demonstrated that the Transformer-based approaches are able to achieve state-of-the-art performance, making

Table 1
Summary of related research work on precipitation nowcasting.

Research	Model	Description	Notable features
Berenguer et al. (2012)	NWP	Physically-based rainfall prediction using atmospheric physics equations	High-resolution forecasts, long lead times
Berenguer et al. (2012), Bech and Chau (2012), Renzullo et al. (2017)	Radar-Based Models (Extrapolation)	Radar data extrapolation for better short-term (0–6 h) rainfall prediction	Improved performance compared to NWP, short lead times
Ayzel et al. (2019)	Optical Flow-Based Model (rainymotion)	Uses optical flow for precipitation nowcasting	Utilizes advanced observation data, open-source Python library
Pulkkinen et al. (2019)	Probabilistic Nowcasting (pySTEPS)	Deterministic and probabilistic nowcasting application	Developed in open-source Python library, applicable in multiple countries
Poletti et al. (2019), Hwang et al. (2020)	NWP-Radar Blending Technique	Combination of NWP and radar-based models for short-term flood forecasting	Improved short-term nowcasting performance
Shi et al. (2015)	ConvLSTM Model	Radar-based model with ConvLSTM architecture for spatiotemporal correlation	Outperforms optical flow-based models in capturing correlations
Agrawal et al. (2019)	U-Net Model	Fully connected CNN model for better predictions	Outperforms traditional NWP models
Isola et al. (2017), Rüttgers et al. (2019)	GAN	GAN and cGAN architectures for image-to-image tasks	Improved image quality
Ravuri et al. (2021)	Video GAN Model	Deep generative model inspired by video GAN for convective cell prediction	Enhances precipitation forecast quality
Tuyen et al. (2022)	U-Net Model and RNN	Precipitation nowcasting with weather radar echo pictures combining the U-Net segmentation model and the PredRNN-v2 DL model	Reduced processing time and prediction error
Ayzel et al. (2020)	CNN	RainNet, a CNN-based model proposed for precipitation nowcasting using radar images	RainNet performs much better than the benchmark models in terms of MAE and CSI

them valuable tools for predicting precipitation in a timely and accurate manner.

As it pertains to precipitation nowcasting, the relationship between the frames of radar echo are crucial to the accuracy of the forecast. It is possible to model these dependencies effectively using transformers, allowing for more accurate predictions to be made. An attention mechanism is employed by them, which enables them to focus on the parts of the input sequence that are relevant to their goal. When it comes to radar echo sequences, this means identifying critical features (such as storm cells) and their evolution over the course of the sequence. Furthermore, Transformers can also make predictions autoregressively, taking into account previously predicted frames, which is essential for maintaining consistency and coherence among predictions. Researchers have demonstrated that Transformer-based models achieve state-of-the-art performance when compared to existing methods, by taking advantage of their ability to provide spatial and temporal information simultaneously, which enables them to achieve state-of-the-art performance.

3. Proposed methodology

Transform-based generative models have revolutionized the process of nowcasting precipitation by effectively capturing temporal dependencies and handling spatial information. Using attention mechanisms inspired by natural language processing, these models, which are based on radar echo sequences, can be used to manipulate critical features in radar echo sequences. As a result of their ability to predict using autoregressive models, they ensure consistency and coherence of their models. According to recent research, Transformer-based approaches can achieve state-of-the-art performance for predicting precipitation, making them valuable tools for predicting precipitation in an accurate and timely manner.

Our objective is to develop a model for precipitation prediction based on nowcasting data that can be used to estimate the urban water supply and prevent floods in dam basins where an accurate rainfall forecasting system is essential for the estimation of urban water supply. Hence, we use a transformer generative model in order to accurately predict precipitation based on raw radar reflective data so that it can be forecasted in advance. Basically, an encoder–decoder structure makes up the Transformer architecture (Chattopadhyay et al., 2022). When it comes to image data, the encoder portion concentrates on obtaining features from the input pictures, while the decoder portion produces outputs or predictions based on these features. Typically, the Transformer model encoder begins with a convolutional backbone, like a CNN that has already been trained (such as ResNet or EfficientNet) (Tuyen et al., 2022). Using convolutional layers, this backbone processes the input image and extracts hierarchical characteristics.

The convolutional layers capture spatial information from the image in order to combine the high-level characteristics of the earlier layers with the low-level features of the deeper layers. Using Transformer layers, the model can capture long-range interactions and global dependencies between patches after patch extraction (Bojesomo et al., 2021). There are three layers in Transformer, each of which is made up of neural networks that feed forward based on position and self-attention processes. A Transformer layer's self-attention mechanism aids in the computation of the relative relevance of various patches or tokens, thus capturing links between visual elements (Vaswani et al., 2017). When extracting features, the model can focus on informative patches and give them more weight.

By adding a decoder layer to the Transformer architecture, the final output is produced (Bojesomo et al., 2021). The decoder uses convolutional layers or upsampling procedures to reconstruct the output image based on the processed information from the Transformer layers. In this architecture, the Transformer model is able to capture both long-range dependencies and global context by leveraging both Transformer attention processes and CNN spatial feature extraction. In order to address the research objectives, this section discusses the step-by-step methodology. The methodology involves data preparation, pre-processing, model development, training, evaluation, and the application of transfer learning concepts.

3.1. Data preparation

3.1.1. Data acquisition

This study focuses on the Soyang Dam basin in South Korea, which is upstream of the Han River. The Soyang Dam basin (delineated as the

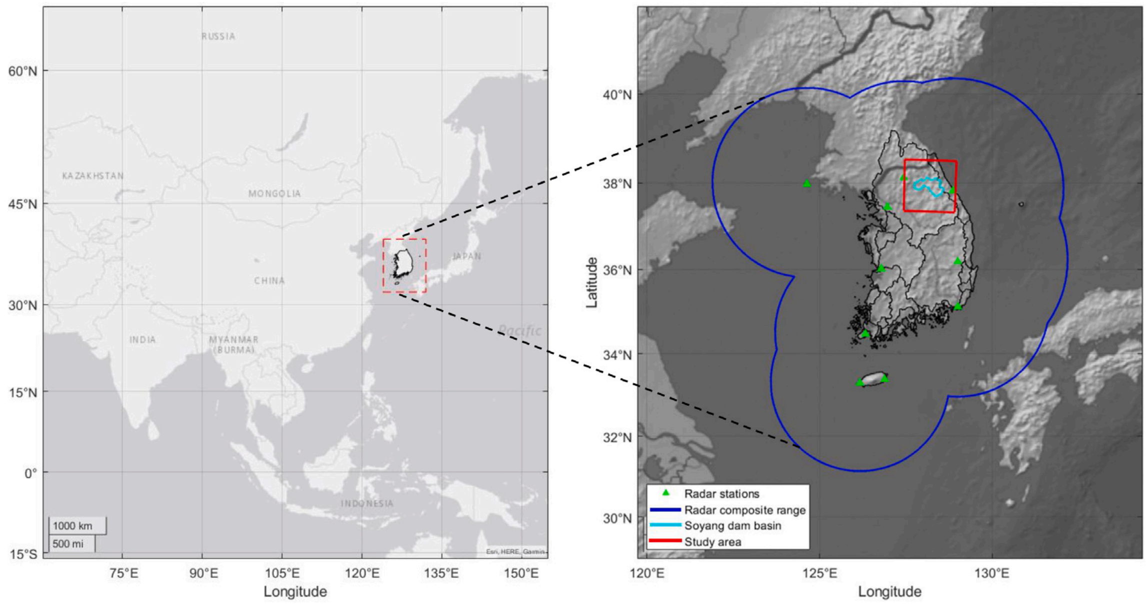

Fig. 1. Study area.

cyan color in Fig. 1, lies within a monsoon climate zone and receives an annual precipitation of approximately 1200 mm. About 70% of the annual precipitation falls during the summer season from June to September, and typhoons often cause significant floods in that season. Soyang Dam plays a crucial role in both water supply and flood control in metropolitan areas, including Seoul.

To develop the precipitation nowcasting model, employ the 1.5 km constant altitude plan position indicator (CAPPI) radar composite dataset from 10 weather radars covering the entire South Korea provided by the Korean Meteorological Administration (KMA). The radar composite dataset is composed of reflectivity in decibels (dBz), with a spatial resolution of 1 km over a 960 × 1200 grid updated every 10 min. The Reflectivity is normalized to a scale between 0 and 1 using the min–max scaler method for model training. The training and test datasets are specifically prepared to include the Soyang Dam basin by cropping into 128 × 128 grids, highlighted as a red square in Fig. 1. The radar composite datasets feature relatively higher rainfall intensities, incorporating extreme rainfall events recorded from the summer of 2018 to 2022. A total of 3092 .npy files are used to collect radar reflectivity data. We divide the data into two categories: training and testing. In the training dataset, 1845 .npy files are measured between June 2014 and August 2017, whereas in the testing dataset, 1247 .npy files are measured between June and August 2018. The reflectivity data is converted into precipitation estimates using the commonly used $Z-R$ relationship equation, as follows.

$$Z = 200R^{1.6}, \tag{1}$$

where Z represents radar reflectivity ($\mathrm{mm^6m^{-3}}$), and R is the precipitation rate ($\mathrm{mmh^{-1}}$) (Choi and Kim, 2022).

Table 2 summarizes statistical data derived from radar reflectivity datasets obtained from 10 weather radar stations situated across South Korea. The most events have relatively high rainfall intensity ($R \geq 20$ mm). The dataset contains 3092 rainfall events, with 1845 events allocated for training and the remaining 1247 events (from 2022) used as the test datasets.

3.2. Data preprocessing

Raw radar reflectivity measurements are typically reported in dBz. These measurements represent the intensity of radar echoes returned from precipitation or other atmospheric phenomena. To transform these measurements into grayscale images, we map the dBz values to pixel intensities ranging from 0 to 255. This mapping allows us to visualize the reflectivity data as shades of gray. The rationale behind using grayscale images is that they provide a straightforward representation of the radar reflectivity patterns.

After converting radar reflectivity data to grayscale, we proceed with normalization. Normalization ensures that all images or data points have the same scale, making them easily comparable. The Min-Max scaler method is commonly used for this purpose. We determine the minimum and maximum values observed in the training dataset. The grayscale values are then rescaled within the range of 0 to 1. By normalizing the grayscale values, we ensure that the entire range of reflectivity data is represented consistently across different images.

Dealing with missing data is crucial in any preprocessing pipeline. When working with radar reflectivity data, we encounter missing values due to various reasons (e.g., radar beam blockage, equipment malfunction, or gaps in coverage). There are common approaches to handle missing data that we apply on our dataset including; (a) Interpolation: If the missing data occurs within a sequence of radar scans, we can interpolate the missing values based on neighboring scans. Linear interpolation or spline-based methods are often used. (b) Masking: We can create a binary mask where missing values are marked as “masked” pixels. During subsequent processing, we exclude these masked pixels from calculations. And (c) Imputation: Imputation techniques (e.g., mean imputation, median imputation, or regression-based imputation) can be used to estimate missing values based on available data.

Table 2
Statistical information of radar reflective dataset collected from 10 weather radars across South Korea.

Precipitation rate	Training data		Testing data	
$0 \leq R < 1$	17	0.9%	1	0.1%
$1 \leq R < 2.5$	46	2.5%	23	1.8%
$2.5 \leq R < 5$	35	1.9%	64	5.1%
$5 \leq R < 10$	154	8.3%	184	14.8%
$10 \leq R < 20$	276	15.0%	298	23.9%
$20 \geq R$	1317	71.4%	677	54.3%
Total	1845	100%	1247	100%

3.3. Input–output data preparation

The input and output data of our Transformer model are carefully structured to facilitate training and evaluation. For input data, we select the four most recent radar reflectivity snapshots at time intervals of $t-30$, $t-20$, $t-10$ minutes, and the current time (t minutes). The radar reflectivity data for 10 min ahead is predicted using this selection. The output data consist of calculated precipitation values derived from the $Z--R$ (reflectivity-to-rainfall) relationship, corresponding to the predictions made by our model.

3.4. Model development

To provide accurate weather predictions, transformers can exploit spatial and temporal dependencies in radar image data. The TensorFlow and Keras libraries are used to construct a Transformer model for precipitation nowcasting. Domain-specific insights guided the exploration and testing of various hyperparameters and architectural configurations to optimize the model's predictive capabilities.

3.4.1. cGAN

A cGAN consists of a generator (G) and a discriminator (D), like traditional GANs, but with a conditioning input that guides the generation process. Generators take both random noise and conditioning information as inputs, and discriminators are trained to differentiate between real and generated samples.

In the paper, we use the cGAN framework for image translation tasks. Especially, G is trained to generate target images of predicted rainfall based on the input images(x) and random noise(z), while D is adversarially trained to discriminate the source of these images which is from real data(y) or fake image from G. The loss function of cGAN architecture as follows.

$$L_{cGAN}(G,D) = E_{x,y}[log D(x,y)] + E_{x,z}[log(1-D(x,G(x,z)))], \tag{2}$$

where losses are calculated as expected (E) values.

Precipitation nowcasting based on U-Net model has previously demonstrated performance superior to that of a traditional radar-based precipitation nowcasting model that uses optical flow. Based on it, we deploy some attention gates to U-Net networks as G to suppress irrelevant areas in the input image and highlight the salient features of specific local areas. To ensure both temporal and spatial consistency, we use the PatchGAN discriminator as D. It is designed in a fully convolutional form, mapping the target image of G to an $N \times N$ matrix rather than just a boolean value. This matrix evaluates different regions of the target image separately to determine the legitimacy of the target image. Hence, we consider to the pixel-level L1-norm loss between generated images $G(x)$ and target images y, as follows.

$$L_{pix}(G) = E_{x,y,z}[\|y - G(x,z)\|_1], \tag{3}$$

where $\|.\|_1$ represents the L1-norm.

In cGAN architecture, the aim of G is to minimize the loss function $L_{cGAN}(G,D)$, by contract, D try to maximize this function. Meanwhile, we combine $L_{pix}(G)$ and $L_{cGAN}(G,D)$ to consider details of images to improve the quality of output. The final target function $G^{\star}$ is expressed as,

$$G^{\star} = L_{cGAN}(G,D) + \lambda \times L_{pix}(G), \tag{4}$$

where λ is a hyperparameter weight that needs to be set.

Algorithm 1: A Minibatch stochastic gradient descent training for cGan-att.

Input: Noise Samples m, Real Samples, Number of Iterations, learning rate, and Momentum

Output: Discriminator Output $D(G(z_i))$, Generator Output $D(G(y_i))$, Updated Discriminator Parameters (θ_d), Updated Generator Parameters (θ_g)

for *Number of training iterations* **do**

Sample minibatch of m noise samples $\{z_1,z_2,\ldots,z_m\}$ from noise prior.

Sample minibatch of m examples $\{x_1,x_2,\ldots,x_m\}$ from data distribution.

Noise samples are processed by a generator and discriminator to obtain output $D(G(z_i))$.

Real samples are processed by discriminators to obtain output $D(G(y_i))$.

Calculate the discriminator loss function L_d,

$$L_d = -\frac{1}{m}\sum_{i=1}^{m}\Big(\log D(y_i) + \log(1 - D(G(z_i)))\Big)$$

Update discriminator parameters through Adam Gradient Descent Algorithm,

$$\theta_d = Adam\Big(\nabla\theta_d(L_d), \theta_d\Big)$$

Calculate the generator loss function L_g,

$$L_g = \frac{1}{m}\sum_{i=1}^{m}\Big(\log 1 - D(G(z_i))\Big)$$

Update generator parameters through Adam Gradient Descent Algorithm,

$$\theta_g = Adam\Big(\nabla\theta_g(L_g), \theta_g\Big)$$

3.4.2. Generator

Compared to the traditional architecture of cGAN generators of rainfall prediction, we add attention gates into the U-Net as a generator for extracting the features of images more efficiently. After extracting different fine-grained feature maps from input, this generator translates them to target images. The two processes are called contracting and expanding, respectively. A G network consists of one input layer, five convolutional layers, two max-pooling layers, two upsampling layers, and one output layer. The size of input images is $128 \times 128 \times 4$, and the size of output images is $128 \times 128 \times 1$. Convolutional layers consist of 1×1 2D convolutions with zero padding, batch normalization, and ReLU activation functions.

As part of the contracting process, the input image is downsampled using 2D max-pooling operations. Following each skip connection, 2×2 2D up-sampling operations are used to produce different level target images. Using attention gates, skip connections concatenated output images that are at the current level of the contracting part and at a lower level of the expanding part to increase the resolution of featured images. After the max-pooling layers of the contracting part and the convolutional layers of the expanding part, a dropout layer with a rate of 0.5 is applied to prevent overfitting. Lastly, the output convolutional layer used a linear function for activation to predict the future radar reflectivity image using a 1×1 2D convolution.

3.4.3. Discriminator

In traditional discriminators, they just judge whether the target image is produced by G or selected from real data, with the bool value of 0 or 1. However, this method cannot accurately determine the temporal and spatial relationships of each part of the image. Therefore, we apply the PatchGAN discriminator as the D of our model to discriminate images at a local level, providing more fine-grained feedback. The network architecture of G includes an input layer, four convolutional layers, and an output layer. The sizes of the input image and the target image are also $128 \times 128 \times 4$ and $128 \times 128 \times 1$. Each convolutional layer consists of 2×2 2D convolution with zero padding, batch normalization, and an activation function of Rectified Linear Unit (ReLU), which was leaky and had a 0.2 slope. Therefore, we segment the image into 64×64 patches to assess its validity. This has brought about more accurate and finer-grained judgment results.

The Transformer model is trained on the prepared training dataset. According to Algorithm 1, in the rain prediction algorithm, input images from the same geographical location have a temporal causal relationship. In addition to these data, the algorithm requires the following inputs. (a) A minibatch of m noise samples, drawn from a noise prior distribution. The generator uses these noise samples as input. (b) Real Samples, which are micro-batches of m examples taken from the actual distribution of data. Both the generator and discriminator are trained using these real samples. And (c) Hyperparameters, such as the number of training iterations (determined by the user), and the Adam Gradient Descent Algorithm parameters (such as learning rates and momentum).

Using the algorithm, we obtain the following outputs: (a) discriminator prediction for each generated sample, which represents the discriminator's estimate of whether the sample is real or fake. b) Generator Output for each real sample represents the discriminator's estimate of whether the real sample is real or not. (c) Updated Discriminator Parameters to minimize discriminator loss using the Adam Gradient Descent Algorithm. And (d) Updated Generator Parameters as the generator's model parameters after applying the Adam Gradient Descent Algorithm.

With this algorithm, we use the cGAN framework to train, using the rainfall amount at the next time step as a condition, to improve the prediction of rainfall at the current time step. As part of the training process, we randomly select a small batch of samples from a noise prior distribution as input and then randomly select another small batch of samples from the real data distribution. The samples are then passed through the generator and discriminator, where the generator produces fake data and the discriminator evaluates the input data's authenticity.

In the next step, we calculate the loss function of the discriminator, which includes judgments on real data as well as judgments on generated data. A gradient descent algorithm is then used to update the discriminator's parameters. By using the Adam gradient descent algorithm, we calculate the generator's loss function, which evaluates the degree to which generated data is judged as real data. Until the preset number of training iterations is reached, the process iterates continuously.

3.5. Model evaluation

A comprehensive evaluation of the testing dataset is conducted following model training. Evaluation metrics include Pearson correlation coefficient, root mean square error (RMSE), Nash–Sutcliffeefficiency (NSE), CSI, and fraction skill scores. Furthermore, results are generated comparing the average verification metrics for 10-minute precipitation predictions produced by Transformer and default models (cGANs, U-Net, convLSTMs, pySTEP) based on evaluation metrics. Model predictions are calculated at 10, 30, and 60-minute intervals to calculate the fraction skill score (FSS).

The calculation formulas for the evaluation indicators are as follows. We used several symbols including n as the sample size, x as the value of the first variable, y as the value of the second variable, $(\hat{y})$ as the predicted value, $(\bar{y})$ as the mean value of the observed values, $Hits$ as the number of correctly predicted events, $Misses$ as the number of incorrectly predicted events, and $FalseAlarms$ as the number of falsely predicted events.

3.6. Model training

- Pearson correlation coefficient (PCC): a statistic used to evaluate the linear relationship between two variables. Data points are compared with straight lines in a scatter plot to measure how closely they are aligned with one another. There is a range of −1 to 1 for the coefficient. Positive values indicate a direct relationship (when one variable increases, the other tends to increase), while negative values suggest an inverse relationship (when one variable increases, the other tends to decrease). It is important to remember that correlation does not imply causation.

$$r = \frac{n(\sum xy) - (\sum x)(\sum y)}{\sqrt{[n\sum x^2 - (\sum x)^2][n\sum y^2 - (\sum y)^2]}}. \tag{5}$$

- RMSE: measures the average difference between predicted and actual values. Calculated by taking the square root of the average of the squared differences between predicted and actual values. Model performance is evaluated by RMSE, where lower values indicate better predictive accuracy.

$$RMSE = \sqrt{\frac{\sum_{i=1}^{n}(y_i - \hat{y}_i)^2}{n}}. \tag{6}$$

- NSE: is used to assess hydrologic model goodness of fit. With values ranging from negative infinity to 1, the NSE measures the accuracy of the model predictions compared to the observed data. NSE values less than 0 indicate that the mean of the observed data is a better predictor than the model. In NSE, the sum of squared differences between observed and simulated values is normalized by the variance of the observed values.

$$NSE = 1 - \frac{\sum_{i=1}^{n}(y_i - \hat{y}i)^2}{\sum i = 1^n (y_i - \bar{y})^2}. \tag{7}$$

- CSI: a performance metric used to evaluate binary classification models, particularly those working with imbalanced data. While penalizing misclassifications, it considers the proportion of successful predictions within a specific class, typically the minority class. By dividing true positives by the sum of true positives and false negatives, CSI represents the model's ability to correctly identify positive instances. When misclassifications are costly and minority classes are of interest, CSI provides a balanced assessment of model performance.

$$CSI = \frac{Hits}{Hits + Misses + FalseAlarms}. \tag{8}$$

- FSS: it is indeed a valuable metric for assessing the performance of predictive models, especially in meteorological forecasting. In spatial verification, FSS is particularly useful in evaluating how well a model predicts a phenomenon's spatial pattern. The FSS is particularly renowned for its ability to produce results that are not only realistic but also physically consistent, which is crucial when generalizing to unseen data. A traditional deep learning method might not account for spatial correlation in the data, resulting in less realistic predictions.

$$FSS = 1 - \frac{\sum_{i=1}^{n}(\hat{y}i - y_i)^2}{\sum i = 1^n (\bar{y} - y_i)^2}. \tag{9}$$

3.7. Transfer learning

In transfer learning, a model that has already learned useful features from a large dataset is adapted or fine-tuned to meet a specific need. The transfer learning method allows us to use the knowledge gained by a pre-trained model on a related but distinct problem domain, instead of training it from scratch. In this way, we can improve the model's performance while saving computational resources. By transferring learning, we can build on existing expertise and adapt it to new situations.

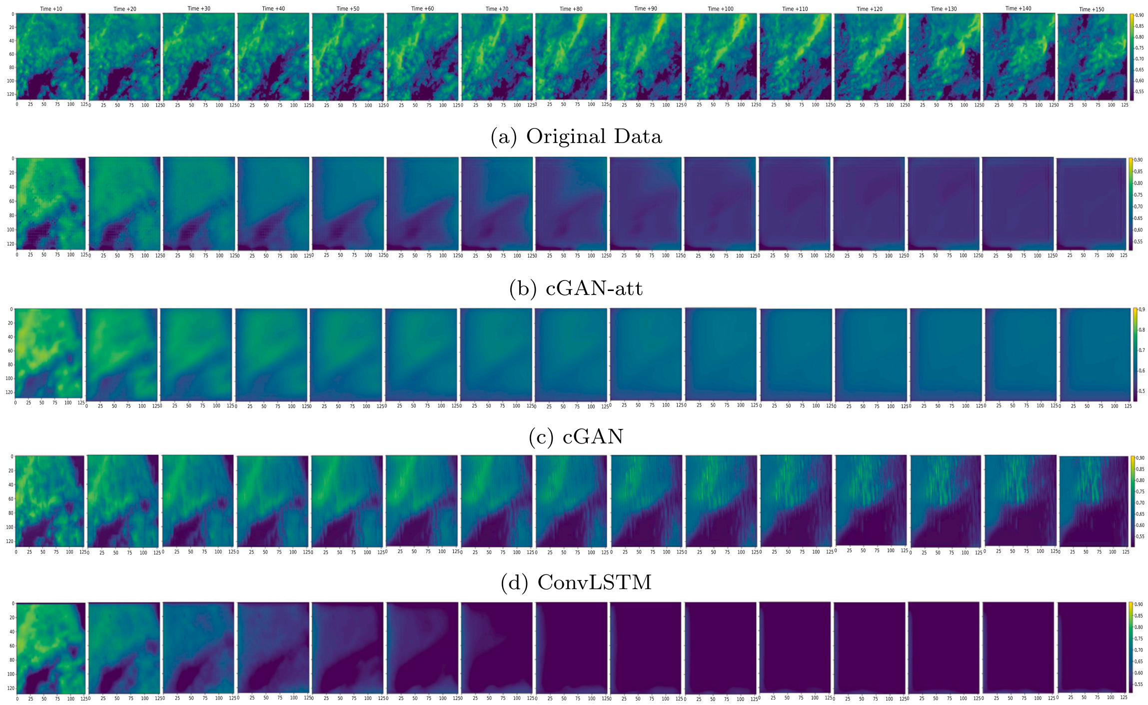

(a) Original Data

(b) cGAN-att

(c) cGAN

(d) ConvLSTM

(e) U-Net

Fig. 2. Model predictions and ground truth for precipitation at different forecast time-frames.

A cost-efficient computational method is then applied to the pre-trained Transformer model to optimize its performance. Modifying pre-trained Transformer models based on radar reflective data for precipitation nowcasting to take advantage of the expertise gathered from models trained on extensive datasets. When transfer learning techniques are applied to pretrained Transformer models, their performance can be greatly enhanced, even with smaller datasets.

4. Experimental results

In this section we present our experimental results for the propsoed model and we compare it with several recent models including cGAN, ConvLSTM, U-Net and pySTEP. In our comparative analysis, we consider prediction accuracy. The results unveil the unique strengths of our proposed model, positioning it as a promising contender in the ever-evolving landscape of Transformers.

In Fig. 2, we showcase the predictions made by our proposed model alongside those of related approaches. Fig. 2.(a) displays a sample of the original dataset, e.g., radar images, that serve as the foundation for our predictions. As we move forward, we will dissect how our model fares against its counterparts.

It is commendable that all schemes remain able to achieve commendable forecast results at Time+10. The cGAN scheme, on the other hand, stands out because it is so ambiguous. In comparison to the actual weather conditions, it appears that the predictions obtained from the cGAN algorithm are the most uncertain. The prediction accuracy of its system, in other words, lags behind its competitors.

This observation is further supported by Figs. 3, 4, 5, 6, and 7. As a matter of fact, the Forecast Skill Score (FSS) value for cGAN consistently remains the lowest as compared to cGan-att, U-Net, and ConvLSTM schemes. In the process of extending predictions further into the future, an interesting phenomenon begins to emerge. In spite of the fact that all models perform well in the beginning, the discrepancies between forecasts and reality gradually increase over time.

This can be attributed to the training process itself, which is the underlying reason. As part of the training process, these schemes rely solely on the rainfall map from the previous time step as an input. With the passage of time, the gap between predictions and actual observations widens, resulting in a gradual decline in the accuracy of prediction as time passes.

The results indicate that ConvLSTM emerges as the champion in terms of prediction performance among the models considered. In order to forecast accurately, it is essential to be able to capture both spatial and temporal dependencies. Another close follow-up is cGan-att, which uses attention mechanisms to enhance context understanding, thus improving performance. Although Gan shows promising signs, ambiguity remains an issue. U-Net's prediction performance, which is known for its semantic segmentation, deteriorates at the fastest rate as time passes.

Basically, we found that our proposed model, with its blend of attention mechanisms and temporal modeling, is able to hold its own against established architectures. As the clock ticks away, the weather unfolds, and our models work tirelessly to unravel its secrets one radar frame at a time, while the clock ticks away.

Table 3 serves as our compass, guiding us through the intricate landscape of predictive prowess. It is the cells that hold the critical metrics that provide insight into the models' performance, much like constellations provide insight into the sky's constellations. The PCC measures the linear relationship between the predicted precipitation value and the actual precipitation value. A higher R-value indicates a stronger alignment between forecasts and reality - a harmonious dance between the two. Our model waltzes gracefully with truth when R flirts with the concept of unity.

It can be thought of as a sentinel guarding against prediction inaccuracies and is similar to the RMSE. As the RMSE value decreases, the precision of the results increases - a bit of a tightrope walk across the data landscape. As we work towards minimizing this error, we are getting closer and closer to the bullseye with our model. It is the NSE that is used to gauge the prowess of our model. There is no doubt that an efficiency value near 1 indicates a well-oiled machine that hums in sync with reality - an efficient machine par excellence. The goal of our model is to find that sweet spot, where efficiency blooms like a rare orchid in the springtime.

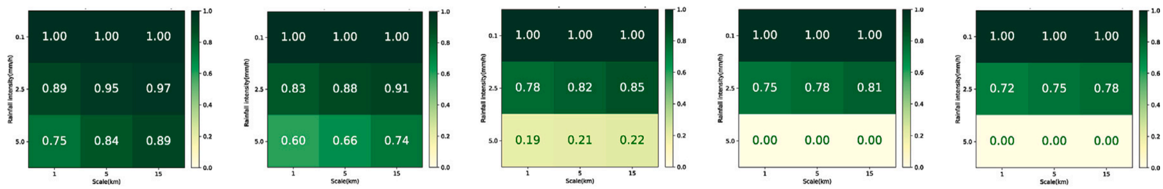

(a) 10-min lead time. (b) 30-min lead time. (c) 60-min lead time. (d) 90-min lead time. (e) 150-min lead time.

Fig. 3. FSS diagram for cGan-att model.

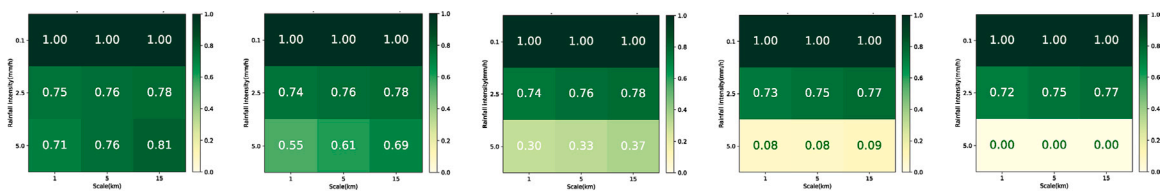

(a) 10-min lead time. (b) 30-min lead time. (c) 60-min lead time. (d) 90-min lead time. (e) 150-min lead time.

Fig. 4. FSS diagram for cGan model.

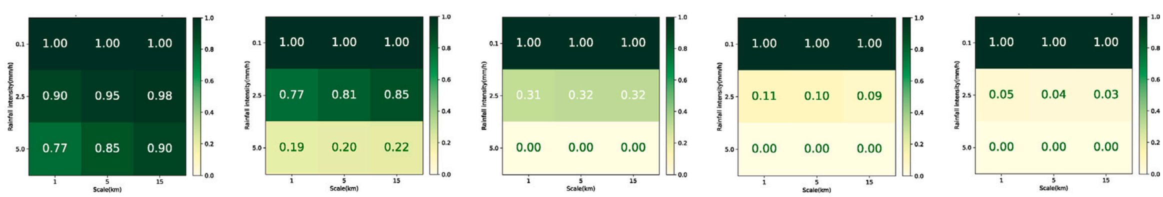

(a) 10-min lead time. (b) 30-min lead time. (c) 60-min lead time. (d) 90-min lead time. (e) 150-min lead time.

Fig. 5. FSS diagram for U-Net model.

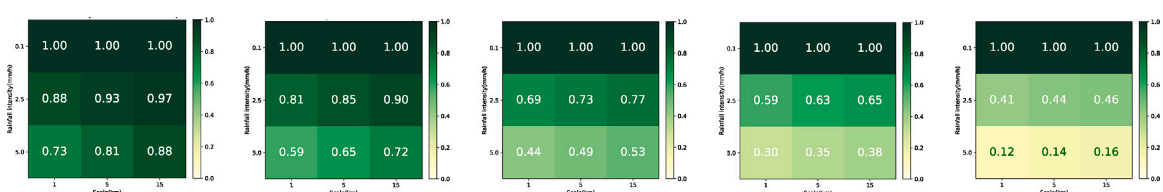

(a) 10-min lead time. (b) 30-min lead time. (c) 60-min lead time. (d) 90-min lead time. (e) 150-min lead time.

Fig. 6. FSS diagram for ConvLSTM model.

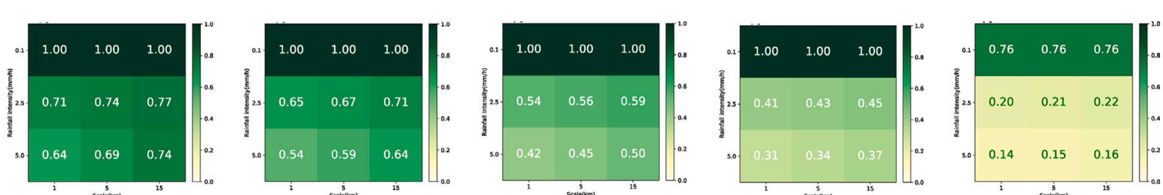

(a) 90-min lead time. (b) 30-min lead time. (c) 60-min lead time. (d) 90-min lead time. (e) 150-min Lead Time.

Fig. 7. FSS diagram for pySTEPS model.

The CSI is described as being the daredevil of metrics, leaping into the fray of extreme events. As a result of this measurement, we can tell how well our model does at predicting those rare, tempestuous downpours. The higher the CSI value, the more bullseyes our model will hit, arrows that will pierce the heart of extreme precipitation from our model. The purpose of this celestial tableau is to compare the strengths, quirks, and alignments of each model with the rest of the universe. As each metric whispers secrets to the model, we are able to discern which one dances gracefully with the data and which one stumbles. So, fellow stargazers, consult Table 3—it holds the keys to our 10-minute precipitation predictions.

5. Discussion

The purpose of this section is to provide a detailed analysis of our experimental findings by carefully analyzing the performance of our proposed model and comparing with the related counterparts. The following is a description of the meteorological script that appears in Table 3.

Specifically, the PCC values (R) for cGan-att and U-Net at $t+10t+10$ minutes are close to unity. As a result of this celestial alignment, their predicted values closely match the observed reality with a remarkable degree of fidelity. Now that we have seen the RMSE, let us take a closer look at it. In the case of cGan-att, this value is negligible, which means

Table 3
Performance comparison of our proposed model compared to related models in terms of 10-Minute Precipitation Prediction.

Metric	cGan-att	cGan	ConvLSTM	U-Net	pySTEPS
R	0.9248	0.9142	0.8882	0.9281	0.7865
$RMSE$	5.9571	9.0944	6.2122	6.1629	16.3699
NSE	0.7343	0.3808	0.7111	0.7157	−1.0062
$CSI(0.1)$	1.0	1.0	1.0	1.0	1.0
$CSI(2.5)$	0.8608	0.6450	0.8490	0.8680	0.6012
$CSI(5.0)$	0.7510	0.6873	0.7200	0.7694	0.5313

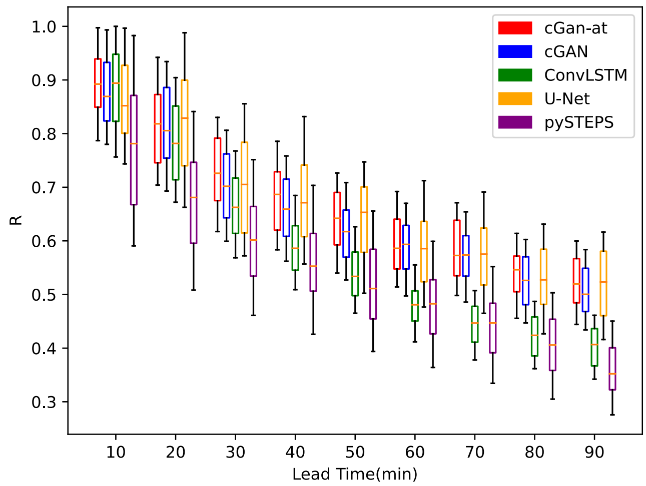

Fig. 8. Comparative analysis of R Values in Box plots: our proposed model vs. related models for up to 90-Minute lead times across Soyang-gang dam basin grids.

that when comparing predicted and actual values, the differences are most likely to exhibit the least dispersion around the mean.

As our trusty compass, the NSE guides us towards the reliability of our models. In this case, cGan-att's NSE value of 1.0 indicates that the company has a high level of reliability and top-tier quality. During a sudden downpour, you had be more likely to trust this umbrella model than your other umbrella models. pySTEPS, on the other hand, hovers around zero while pySTEPS hovers around 1. In spite of the fact that the simulation results are in close alignment with observations, there is a hiccup in the weather crystal ball thanks to a simulation error in the process.

Let us consider rainfall thresholds: At 0.1 mm/h, all schemes achieve a perfect score of 1.0 - like synchronized raindrops in a poetic downpour of rain. At a threshold of 2.5 mm/h, both cGan and pySTEPS seem to stumble a little bit, and their predictions begin to falter a little bit. It is at a more demanding threshold of 5.0 mm/h that both cGan-att and U-Net really excel, boasting the best CSI.

A symphony of precision accompanies cGan-att's performance as we look forward to the future. U-Net follows suit, leveraging its semantic segmentation expertise. In both spatial and temporal dimensions, ConvLSTM waltzes with grace. In spite of the fact that cGan is not flawless, it still possesses the power of prediction. In spite of its best efforts, pySTEPS stumbles - a weather oracle with cloudy predictions.

Fig. 8, and Fig. 9, and Fig. 10 present comparative analysis of R, RMSE, NSE, values in Box plots, respectively. For up to 90-Minute lead times across the grids of the Soyang-gang dam basin, we compare the performance of our proposed model with that of several related models such as cGAN, ConvLSTM, U-Net, and PySTEP. In the 90-minute forecast, it can be seen that all models except PySTEPS have similar performance when it comes to the 90-minute forecast. As a matter of fact, cGan-att performs better than cGAN and U-Net in terms of R, RMSE, and NSE, indicating improvement of cGan-att over cGAN in terms of these metrics.

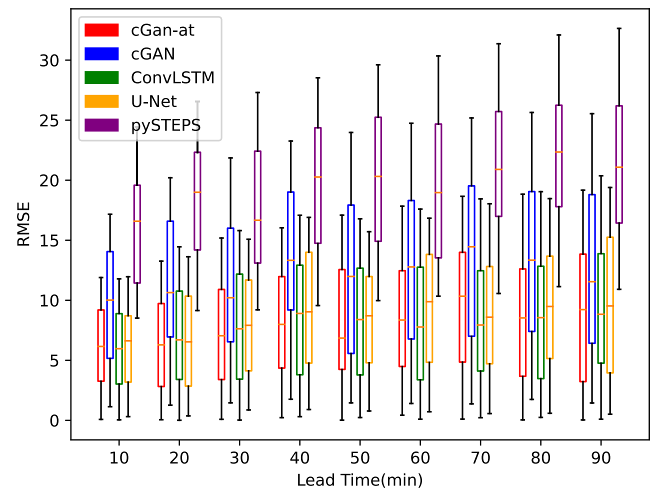

Fig. 9. Comparative analysis of RMSE Values in Box plots: our proposed model vs. related models for up to 90-Minute lead times across Soyang-gang dam basin grids.

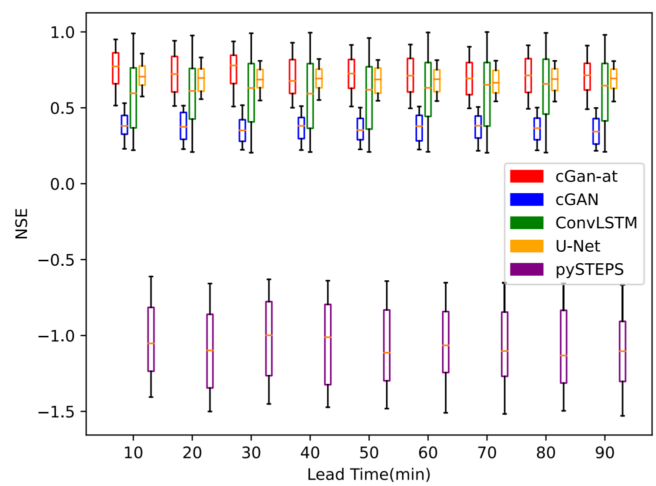

Fig. 10. Comparative analysis of NSe Values in Box plots: our proposed model vs. related models for up to 90-Minute lead times across Soyang-gang dam basin grids.

It can be attributed to the attention mechanism incorporated in cGan-att that explains the superior performance of cGan-att over cGAN in the 90-minute forecast. As a result of this attention mechanism, the forecasting model is able to focus on relevant portions of the input data, effectively capturing key spatial and temporal patterns in the forecasted variable according to the input data. In comparison to cGANs and U-Net, this results in more accurate predictions and better overall performance compared to cGANs and U-Net. Moreover, the results of the study indicate that despite the fact that pySTEPS did not perform as well as the other models in the 90-minute forecast, it is still capable of producing results that are competitive. It is important to note that different models may perform better in different forecast scenarios, and a combination of multiple models may potentially improve the accuracy of forecasts in general.

6. Conclusion and future work

A novel Transformer generative model for precipitation nowcasting was presented in this paper. We proposed a model for predicting precipitation using radar reflectivity data, enabling short-term weather forecasts that are accurate and rapid. The intricate spatial and temporal correlations present in radar reflectivity data align well with the strengths of transformers, enhancing the accuracy of precipitation predictions. We boosted performance effectively by using transfer learning with pre-trained Transformer models. First, we trained the model using a comprehensive dataset. Our study area was Soyang Dam basin in south Korea. We collected radar reflective data from 10 radar stations located across South Korea. Then, we fine-tuned it for precipitation nowcasting using radar reflective data. This adaptation improved the accuracy of rainfall forecasting by capturing crucial features. Leveraging prior task knowledge through transfer learning not only enhanced prediction accuracy but also increased overall efficiency. Through extensive experimental results, we demonstrated that our model outperformed existing weather forecasting methods including cGAN, ConvLSTM, U-Net, and pySTEPS in terms of forecasting accuracy, making it a significant advancement for disaster preparedness and response through improved weather prediction.

We have found that different regions may exhibit significant variations in the frequency, intensity, and duration of rainfall due to varying climatic conditions. Additionally, the resolution of radar data can impact the model's ability to capture rainfall patterns accurately. In the future, we plan to develop rainfall prediction models that can adapt to different climatic conditions by incorporating climate data such as temperature and humidity into the model. We will explore how to use this information to adjust the model's parameters or structure, ensuring it can accurately predict rainfall in various geographical regions. Furthermore, we will develop multi-scale rainfall prediction models capable of handling different radar data resolutions. This will involve effectively integrating or transforming radar data of various resolutions to enhance the model's adaptability to low-resolution data and ensure accurate predictions across different resolutions.

CRediT authorship contribution statement

Md. Jalil Piran: Writing – review & editing, Writing – original draft, Visualization, Validation, Software, Resources, Project administration, Methodology, Investigation, Funding acquisition, Formal analysis, Conceptualization. **Xiaoding Wang:** Writing – original draft, Visualization, Validation, Software. **Ho Jun Kim:** Writing – original draft, Funding acquisition, Formal analysis, Data curation, Conceptualization. **Hyun Han Kwon:** Supervision, Funding acquisition, Formal analysis, Data curation, Conceptualization.

Declaration of competing interest

The authors declare the following financial interests/personal relationships which may be considered as potential competing interests: Hyun Han Kwon reports financial support was provided by Korea Ministry of the Interior and Safety. If there are other authors, they declare that they have no known competing financial interests or personal relationships that could have appeared to influence the work reported in this paper.

Data availability

No data was used for the research described in the article.

Acknowledgments

This work was supported by Korea Environment Industry & Technology Institute (KEITI) through Aquatic Ecosystem Conservation Research Program, funded by Korea Ministry of Environment(MOE), (RS-2021-KE001393).

References

Agrawal, S., Barrington, L., Bromberg, C., Burge, J., Gazen, C., Hickey, J., 2019. Machine learning for precipitation nowcasting from radar images. arXiv preprint arXiv:1912.12132.

Ahamed, A., Bolten, J.D., 2017. A MODIS-based automated flood monitoring system for southeast Asia. Int. J. App. Earth Obs. Geol. 61, 104–117.

Ahmed, M., Tanyas, H., Huser, R., Dahal, A., Titti, G., Borgatti, L., Francioni, M., Lombardo, L., 2023. Dynamic rainfall-induced landslide susceptibility: a step towards a unified forecasting system. Int. J. App. Earth Obs. Geol. 125, 103593.

Akwensi, P.H., Wang, R., Guo, B., 2024. Preformer: A memory-efficient transformer for point cloud semantic segmentation. Int. J. Appl. Earth Obs. Geol. 128, 103730.

Ayzel, G., Heistermann, M., Winterrath, T., 2019. Optical flow models as an open benchmark for radar-based precipitation nowcasting (rainymotion v0. 1). Geol. Mod. Dev. 12 (4), 1387–1402.

Ayzel, G., Scheffer, T., Heistermann, M., 2020. RainNet v1. 0: a convolutional neural network for radar-based precipitation nowcasting. Geol. Mod. Dev. 13 (6), 2631–2644.

Bech, J., Chau, J.L., 2012. Doppler Radar Observations: Weather Radar, Wind Profiler, Ionospheric Radar, and Other Advanced Applications. BoD–Books on Demand.

Berenguer, M., Surcel, M., Zawadzki, I., Xue, M., Kong, F., 2012. The diurnal cycle of precipitation from continental radar mosaics and numerical weather prediction models. Part II: Intercomparison among numerical models and with nowcasting. Mon. Weather Rev. 140 (8), 2689–2705.

Bojesomo, A., Al-Marzouqi, H., Liatsis, P., 2021. Spatiotemporal vision transformer for short time weather forecasting. In: IEEE Int. Confe. on Big Data. IEEE, pp. 5741–5746.

Butsch, C., Beckers, L.-M., Nilson, E., Frassl, M., Brennholt, N., Kwiatkowski, R., Söder, M., 2023. Health impacts of extreme weather events–Cascading risks in a changing climate. J. Health Monit. 8 (Suppl 4), 33.

Cao, Y., Zhang, D., Zheng, X., Shan, H., Zhang, J., 2023. Mutual information boosted precipitation nowcasting from radar images. Remot. Sens. 15 (6), 1639.

Chattopadhyay, A., Mustafa, M., Hassanzadeh, P., Bach, E., Kashinath, K., 2022. Towards physics-inspired data-driven weather forecasting: integrating data assimilation with a deep spatial-transformer-based U-NET in a case study with ERA5. Geol. Mod. Dev. 15 (5), 2221–2237.

Choi, S., Kim, Y., 2022. Rad-cGAN v1. 0: Radar-based precipitation nowcasting model with conditional generative adversarial networks for multiple dam domains. Geol. Mod. Dev. 15 (15), 5967–5985.

Dinh, T.L., Phung, D.K., Kim, S.H., Bae, D.H., 2023. A new approach for quantitative precipitation estimation from radar reflectivity using a gated recurrent unit network. J. Hydrol. 624, 129887.

Fraser, A., Pelling, M., Scolobig, A., Mavrogenis, S., 2020. Relating root causes to local risk conditions: A comparative study of the institutional pathways to small-scale disasters in three urban flood contexts. Glob. Environ. Chan. 63, 102102.

Guo, Y., Xiao, Y., Hao, F., Zhang, X., Chen, J., de Beurs, K., He, Y., Fu, Y.H., 2023. Comparison of different machine learning algorithms for predicting maize grain yield using UAV-based hyperspectral images. Int. J. App. Earth Obs. Geol. 124, 103528.

Hwang, S., Yoon, J., Kang, N., Lee, D.-R., 2020. Development of flood forecasting system on city· mountains· small river area in Korea and assessment of forecast accuracy. J. Korea Wat. Res. Assoc. 53 (3), 225–236.

Isola, P., Zhu, J.-Y., Zhou, T., Efros, A.A., 2017. Image-to-image translation with conditional adversarial networks. In: Proc. of the IEEE Conf. on Comp. Vis. and Pat. Rec.. pp. 1125–1134.

Khankeshizadeh, E., Mohammadzadeh, A., Arefi, H., Mohsenifar, A., Pirasteh, S., Fan, E., Li, H., Li, J., 2024. A novel weighted ensemble transferred U-net based model (WETUM) for post-earthquake building damage assessment from UAV data: A comparison of deep learning-and machine learning-based approaches. IEEE Trans. Geosci. Remote Sens..

Li, W., Zhu, J., Pirasteh, S., Zhu, Q., Fu, L., Wu, J., Hu, Y., Dehbi, Y., 2022. Investigations of disaster information representation from a geospatial perspective: Progress, challenges and recommendations. Trans. GIS 26 (3), 1376–1398.

Poletti, M.L., Silvestro, F., Davolio, S., Pignone, F., Rebora, N., 2019. Using nowcasting technique and data assimilation in a meteorological model to improve very short range hydrological forecasts. Hydro. and Earth Syst. Sci. 23 (9), 3823–3841.

Pulkkinen, S., Nerini, D., Pérez Hortal, A.A., Velasco-Forero, C., Seed, A., Germann, U., Foresti, L., 2019. Pysteps: An open-source Python library for probabilistic precipitation nowcasting (v1. 0). Geol. Mod. Dev. 12 (10), 4185–4219.

Ravuri, S., Lenc, K., Willson, M., Kangin, D., Lam, R., Mirowski, P., Fitzsimons, M., Athanassiadou, M., Kashem, S., Madge, S., et al., 2021. Skilful precipitation nowcasting using deep generative models of radar. Nature 597 (7878), 672–677.

Renzullo, L., Velasco-Forero, C., Seed, A., 2017. Blending radar, NWP and satellite data for real-time ensemble rainfall analysis: a scale-dependent method. Technical Report, Tech. Rep. EP174236, CSIRO, https://doi.org/10.4225/08/594eb78c96025.

Rothman, D., 2021. Transformers for Natural Language Processing: Build Innovative Deep Neural Network Architectures for NLP with Python, PyTorch, TensorFlow, BERT, RoBERTa, and More. Packt Publishing Ltd.

Rüttgers, M., Lee, S., Jeon, S., You, D., 2019. Prediction of a typhoon track using a generative adversarial network and satellite images. Sci. Rep. 9 (1), 6057.

Schmid, F., Wang, Y., Harou, A., 2019. Nowcasting guidelines—A summary. Bulletin 68, 2.

Shi, X., Chen, Z., Wang, H., Yeung, D.Y., Wong, W.K., Woo, W.c., 2015. Convolutional LSTM network: A machine learning approach for precipitation nowcasting. Adv. Neural Inf. Process. Syst. 28.

Trebing, K., Stańczyk, T., Mehrkanoon, S., 2021. SmaAt-UNet: precipitation nowcasting using a small attention-UNet architecture. Pattern Recognit. Lett. 145, 178–186.

Tuyen, D.N., Tuan, T.M., Le, X.-H., Tung, N.T., Chau, T.K., Van Hai, P., Gerogiannis, V.C., Son, L.H., 2022. RainPredRNN: A new approach for precipitation nowcasting with weather radar echo images based on deep learning. Axioms 11 (3), 107.

Vaswani, A., Shazeer, N., Parmar, N., Uszkoreit, J., Jones, L., Gomez, A.N., Kaiser, Ł., Polosukhin, I., 2017. Attention is all you need. Adv. Neural Inf. Process. Syst. 30.

Zannah, R., Bashar, M., Mushfiq, R.B., Chakrabarty, A., Hossain, S., Jung, Y.J., 2024. Semantic segmentation on panoramic dental X-ray images using U-net architectures. IEEE Access 12, 44598–44612. http://dx.doi.org/10.1109/ACCESS.2024.3380027.

Zhang, Y., Long, M., Chen, K., Xing, L., Jin, R., Jordan, M.I., Wang, J., 2023. Skilful nowcasting of extreme precipitation with NowcastNet. Nature 619 (7970), 526–532.

Zhao, Z., Dong, X., Wang, Y., Hu, C., 2024. Advancing realistic precipitation nowcasting with a spatiotemporal transformer-based denoising diffusion model. IEEE Trans. Geosci. Remote Sens..

Zhu, Q., Chen, L., Hu, H., Pirasteh, S., Li, H., Xie, X., 2020. Unsupervised feature learning to improve transferability of landslide susceptibility representations. IEEE J. Sel. Top. App. Earth Observ. and Rmt Sens. 13, 3917–3930.